Multiomics profiling of human plasma and CSF reveals ATN derived networks and highlights causal links in Alzheimer's disease

Liu Shi[a+], Jin Xu[b+], Rebecca Green[c,d,e], Asger Wretlind[f], Jan Homann[g], Noel J. Buckley[a], Betty M. Tijms[h], Stephanie J. B. Vos[i], Mara ten Kate[h], Sebastiaan Engelborghs[j,k], Kristel Sleegers[l,m], Giovanni B. Frisoni[n,o], Anders Wallin[p], Alberto Lleó[q], Julius Pop[r,s], Pablo Martinez-Lage[t], Johannes Streffer[u], Frederik Barkhof[v,w], Henrik Zetterberg[x,y,z,aa], Pieter Jelle Visser[h,i], Simon Lovestone[a,bb], Lars Bertram[g,cc], Alejo J. Nevado-Holgado[a], Petroula Proitsi[c*], Cristina Legido-Quigley[b,f*]

[a] Department of Psychiatry, University of Oxford, UK
[b] Institute of Pharmaceutical Science, King's College London, London, UK
[c] Institute of Psychiatry, Psychology & Neuroscience, King's College London, London, UK
[d] UK National Institute for Health Research (NIHR) Maudsley Biomedical Research Centre, South London and Maudsley Trust, London, UK
[e] MRC Unit for Lifelong Health & Ageing at UCL, University College London, London, UK
[f] Steno Diabetes Center Copenhagen, Gentofte, Denmark
[g] Lübeck Interdisciplinary Platform for Genome Analytics, Institutes of Neurogenetics and Cardiogenetics, University of Lübeck, Lübeck, Germany
[h] Alzheimer Center, VU University Medical Center, Amsterdam, the Netherlands
[i] Department of Psychiatry and Neuropsychology, School for Mental Health and Neuroscience, Alzheimer Centrum Limburg, Maastricht University, Maastricht, the Netherlands
[j] Reference Center for Biological Markers of Dementia (BIODEM), Institute Born-Bunge, University of Antwerp, Antwerp, Belgium
[k] Department of Neurology, UZ Brussel and Center for Neurociences (C4N), Vrije Universiteit Brussel, Brussels, Belgium
[l] Complex Genetics Group, VIB Center for Molecular Neurology, VIB, Antwerp, Belgium
[m] Institute Born-Bunge, Department of Biomedical Sciences, University of Antwerp, Antwerp, Belgium
[n] University of Geneva, Geneva, Switzerland
[o] IRCCS Istituto Centro San Giovanni di Dio Fatebenefratelli, Brescia, Italy
[p] Institute of Neuroscience and Physiology, Sahlgrenska Academy at University of Gothenburg, Gothenburg, Sweden
[q] Neurology Department, Hospital Sant Pau, Barcelona, Spain. Centro de Investigación en Red en enfermedades neurodegenerativas (CIBERNED).
[r] University Hospital of Lausanne, Lausanne, Switzerland
[s] Geriatric Psychiatry, Department of Mental Health and Psychiatry, Geneva university Hospitals, Geneva, Switzerland
[t] CITA-Alzheimer Foundation, San Sebastian, Spain
[u] AC Immune SA, Lausanne, Switzerland, formerly Janssen R&D, LLC. Beerse, Belgium at the time of study conduct
[v] Department of Radiology and Nuclear Medicine, Amsterdam UMC, Vrije Universiteit, The Netherland
[w] Queen Square Institute of Neurology and Centre for Medical Image Computing, University College London, UK
[x] Clinical Neurochemistry Laboratory, Sahlgrenska University Hospital, Mölndal, Sweden
[y] Department of Psychiatry and Neurochemistry, Institute of Neuroscience and Physiology, Sahlgrenska Academy, University of Gothenburg, Mölndal, Sweden
[z] UK Dementia Research Institute at UCL, London, United Kingdom
[aa] Department of Neurodegenerative Disease, UCL Institute of Neurology, London, United Kingdom
[bb] Janssen Medical (UK), High Wycombe, UK

[cc] Department of Psychology, University of Oslo, Oslo, Norway

+ contributed equally
*** Correspondence:**
Cristina Legido Quigley: cristina.legido_quigley@kcl.ac.uk
Petroula Proitsi: petroula.proitsi@kcl.ac.uk

Abstract (150 words limit)

INTRODUCTION: This study employed an integrative system and causal inference approach to explore molecular signatures in blood and CSF, the Amyloid/Tau/Neurodegeneration [AT(N)] framework, MCI conversion to AD, and genetic risk for AD.

METHODS: Using the EMIF-AD MBD cohort, we measured 696 proteins in cerebrospinal fluid (n=371), 4001 proteins in plasma (n=972), 611 metabolites in plasma (n=696) and genotyped data in whole-blood (7,778,465 autosomal SNPs, n=936). We investigated associations: molecular modules to AT(N), module hubs with AD Polygenic Risk scores and APOE4 genotypes, molecular hubs to MCI conversion and probed for causality with AD using Mendelian Randomization (MR).

RESULTS: AT(N) framework associated key hubs were mostly proteins and few lipids. In MR analyses, Proprotein Convertase Subtilisin/Kexin Type 7 showed weak causal associations with AD, and AD was causally associated with Reticulocalbin 2 and sphingomyelins.

DISCUSSION: This study reveals multi-omics networks associated with AT(N) and MCI conversion and highlights AD causal candidates.

Key words: Alzheimer's disease; multi-omics; AT(N) framework; polygenic risk score; Mendelian randomization; multimodal biomarker

1. Introduction

77 Alzheimer's disease (AD) is characterised by the presence of β-amyloid (Aβ) containing plaques, and
78 neurofibrillary tangles composed of modified tau protein together with the progressive loss of
79 synapses and neurons [1]. The National Institute on Aging and Alzheimer's Association (NIA-AA) have
80 proposed to classify AD based on biomarkers of amyloid pathology (A), tau pathology (T), and
81 neurodegeneration (N) (the ATN framework) [2]. Yet, despite their diagnostic utility, these three
82 markers reflect only a portion of the complex pathophysiology of AD. In prodromal stages, the
83 interplay between AT(N) changes, genetic factors and peripheral molecular changes may affect the
84 rate of disease progression.

85 Conducting unbiased and high-throughput omics-based research in biological fluids and human brain
86 tissues provides a data-driven approach to identify the many processes involved in AD pathogenesis
87 and to prioritize links to relevant clinical and neuropathological traits. For example, an increasing
88 number of proteomics studies [3-5], including ours [6-8], have identified AD pathophysiological
89 pathways related to immune response and inflammation, oxidative stress, energy metabolism and
90 mitochondrial function. Metabolomics studies have also identified such pathways related to AD [9-
91 11]. A combination of omics, also called multi-omics or deep phenotyping studies, provides an
92 opportunity to explore the molecular interplay with both genotypic and phenotypic variability in AD,
93 bringing in new findings and uncovering novel pathways. Finally, causal inferences approaches allow
94 to scrutinize the causal relationship between molecular markers and AD, highlighting potential
95 interventional targets. Therefore, in this study, we conducted multi-omics analyses with four
96 modalities (cerebrospinal fluid [CSF] proteomics, plasma proteomics, plasma metabolomics and
97 whole blood genetics) from the EMIF-AD MBD study, followed by Mendelian Randomization (MR)
98 analyses (**Figure 1**).

99 We have four objectives: Firstly, we wanted to test if proteomic and metabolomic molecular
100 signatures were associated with AD endophenotypes including amyloid, CSF total tau (T-tau), CSF
101 phosphorylated tau (P-tau), white matter hyperintensity volume, CSF YKL-40, mini mental state

102 examination (MMSE) score, and mild cognitive impairment (MCI) conversion. Secondly, we wanted
103 to investigate the associations between molecular signatures and molecular hubs (main molecules
104 driving associations) with APOE4 genotypes and AD polygenic risk scores (PRS). Thirdly, we wanted
105 to query our findings in prodromal AD by extracting and integrating hub molecules in MCI individuals
106 that converted to AD by computing a network for MCI converters versus non-converters. Finally, MR
107 analyses interrogated the causal relationship between hub molecules and AD.

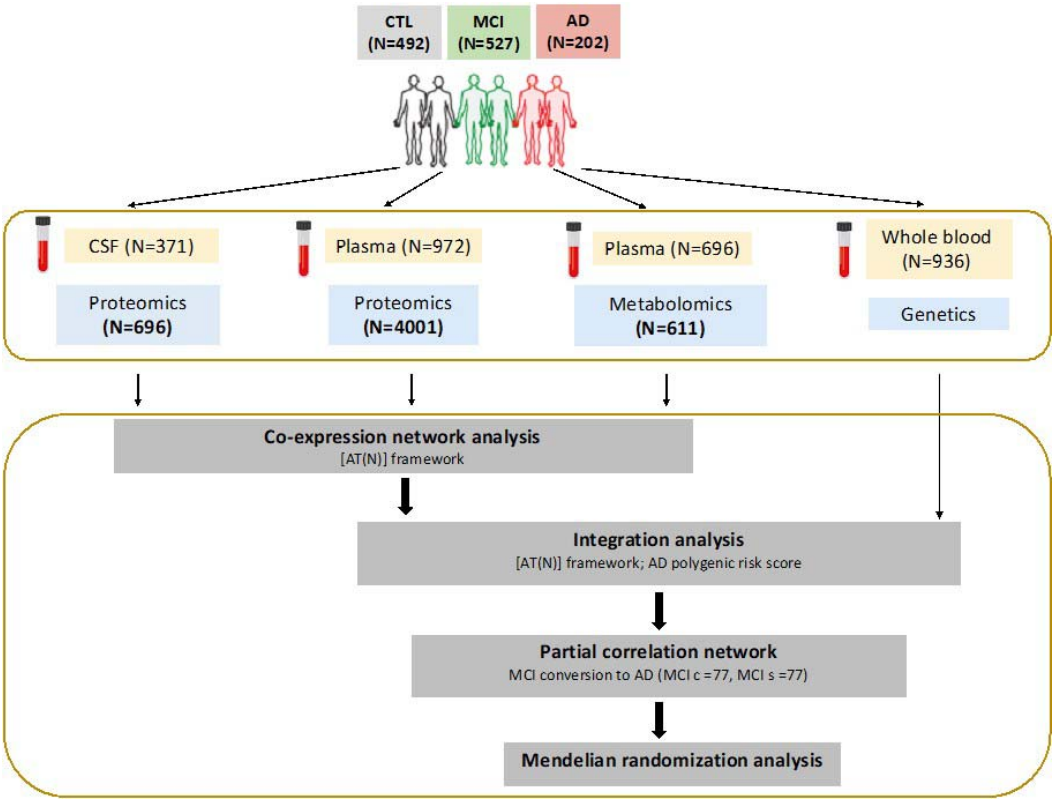

108 **Figure 1. Flowchart of study design.** CTL, cognitively normal controls; MCI, mild cognitive
109 impairment; AD, Alzheimer's disease; Aβ, β-amyloid; CSF, cerebrospinal fluid; A, amyloid pathology;
110 T, tau pathology; N, neurodegeneration; PRS, polygenic risk score; MR, mendelian randomization.

111

112 **2. Methods**

113 **2.1. Participants: EMIF-AD Multimodal Biomarker Discovery (MBD) study**

114 The EMIF-AD MBD study is part of the European Medical Information Framework for Alzheimer's
115 disease (EMIF; http://www.emif.eu/emif-ad-2/); a public-private partnership funded through the

116 Innovative Medicines Initiative (IMI). The design of the EMIF-AD MBD study has been described
117 previously [12]. Briefly, 1221 samples from three groups of people (cognitively normal controls [CTL],
118 MCI and AD) were chosen from pre-existing cohorts with the goal of including samples from people
119 with pathology as well as those without. All participating centres have agreed to share data as part
120 of the EMIF-AD MBD study.

121 General clinical and demographic information were available for all subjects (including *APOE* ε4
122 genotype data). Furthermore, each participant had a measure of brain amyloid load, using either CSF
123 Aβ or amyloid positron emission tomography (PET) imaging. CSF T-tau and P-tau analysis data were
124 available for over 90% of the subjects. We used CSF (or where not available, PET) amyloid as "A", CSF
125 P-tau 181 as "T" and CSF T-tau as "N" to define the AT(N) framework. The classification of the status
126 (abnormal/normal) of amyloid, P-tau and T-tau has been described previously [12]. We
127 dichotomized these biomarkers as normal or abnormal and categorized them into four groups: no
128 pathology (A-T-N-, referring as "A-TN-"), amyloid positive but both T and N negative (A+T-N-,
129 referring as "A+TN-"), amyloid positive and T/N positive (including A+T-N+, A+T+N- and A+T+N+,
130 referring as "A+TN+") and Suspected Non-Alzheimer Pathology (SNAP, including A-T-N+, A-T+N- and
131 A-T+N+). In addition, the following AD-related endophenotypes were also measured for the majority
132 of the subjects: (i) CSF YKL-40; (ii) MRI measures of white matter hyperintensities; (iii) clinical
133 assessments including baseline diagnosis, baseline MMSE score and MCI conversion [12].

134 **2.2. Omics analyses**

135 We performed multi-omics analyses for these subjects including CSF proteomics, plasma proteomics
136 and metabolomics as well as genome-wide SNP genotyping analyses (**Figure 1**).

137 *CSF proteomics*

138 We used tandem mass tag (TMT) technique to measure proteins in CSF. More details can be found in
139 [13]. We imputed proteins using K-nearest neighbour (K=10) and removed any missing > 70%,
140 leading to a total of 696 proteins in 371 samples for further analysis.

141 *Plasma proteomics*

142 We used the SOMAscan assay platform (SomaLogic Inc.) to measure proteins in plasma. SOMAscan
143 is an aptamer-based assay allowing for the simultaneous measurement and quantification of large
144 number of proteins. Here we measured 4001 proteins in 972 individuals. The details have been
145 described previously [14].

146 *Plasma metabolomics*

147 We measured plasma metabolites using Metabolon platform (Metabolon Inc.). Metabolites with
148 more than 70% missing were excluded and we imputed the missing metabolites using K-nearest
149 neighbour (K=10), resulting in 611 metabolites in 696 subjects for further analysis. More details can
150 be found in [11].

151 *Single nucleotide polymorphism (SNP) genotyping*

152 A detailed account of the genotyping procedures and subsequent bioinformatic workflows can be
153 found in [15]. Briefly, a total of 936 DNA samples were sent for genome-wide SNP genotyping using
154 the Infinium Global Screening Array (GSA) with Shared Custom Content (Illumina Inc.). After quality
155 control (QC) and imputation, a total of 7,778,465 autosomal SNPs with minor allele frequency (MAF)
156 ≥0.01 were retained in 898 individuals of European ancestry for downstream analyses and genetic
157 principal components (PCs) were computed [15].

158 **2.3. Statistical analysis**

159 All statistical analyses were completed using R (version 4.1.2). To compare baseline cohort
160 characteristics across three different diagnostic groups (CTL, MCI and AD), we used one-way analysis
161 of variance (ANOVA) and chi-square tests to compare continuous and binary variables, respectively.

162 *Weighted Gene Correlation Network Analysis (WGCNA)*

163 We used the R package WGCNA [16] to construct a weighted and unsigned co-expression network
164 for each individual omics layer. This clustering method is based on calculating correlations between
165 paired variables. The resulting modules or groups of co-expressed analytes were used to calculate
166 module eigenprotein/eigenmetabolite metrics. The eigenprotein/eigenmetabolite-based
167 connectivity (kME) value was used to represent the strength of an analyte's correlation with the
168 module. Analytes with high intramodular kME in the top 90th percentile within a module were
169 considered as hub proteins/metabolites.

170 The correlations between eigenprotein/eigenmetabolite and AD endophenotypes were calculated
171 using Spearman's correlation, the *p* values were corrected with false discovery rate (FDR) and
172 corrected *p* values are presented in a heat map. Furthermore, we used one way ANOVA test to
173 assess pairwise difference of eigenprotein/eigenmetabolite among different AT(N) framework.

174 *Pathway enrichment analysis*

175 Protein pathway enrichment analysis was performed using WebGestalt software
176 (http://www.webgestalt.org/). Briefly, proteins within a module were assembled into a "protein list"
177 and all proteins measured were used as "background". This enrichment analysis was performed on
178 the KEGG database. Metabolite enrichment analysis was performed using the hypergeometric test.
179 The original 60 sub-pathways pre-defined by Metabolon based on the KEGG database were
180 employed as reference [17]. We further performed cell type enrichment analysis for CSF proteins
181 using BEST tool (http://best.psych.ac.cn/#).

182 *AD polygenic risk score (PRS) calculation*

183 The genome-wide association study summary statistics from Kunkle et al. [18] (N=63,926; 21,982 AD
184 clinically ascertained cases, 41,944 controls) were used as the reference data. PRS were constructed
185 using PRSice-2 [19], with and without SNPs in the *APOE* region (chr 19, GRCh37 coordinates

186 44912079 to 45912079) [20]. AD PRS were computed using two p-value thresholds (P_T), previously
187 recommended for PRS including and excluding the *APOE* region: $5x10^{-8}$ (*APOE* region included) and
188 0.1 (*APOE* region excluded) [21]. SNPs in linkage disequilibrium (r2>0.001 within a 250kb window)
189 were clumped, retaining the SNP with the lowest *p*-value.

190 *Association of AD PRS and AT(N) with modules and hubs*

191 We used linear regression analyses to investigate the association of AD PRS (as predictor) with
192 eigenprotein/eigenmetabolite of AT(N) framework-related modules and hub proteins/metabolites
193 (with kME varying from top 90th percentile to top 98th percentile) in these modules, adjusting for
194 sex, age, and genetic PC1 to PC5 [22] (to control for population stratification). We used logistic
195 regression analyses to explore the association of AT(N) markers (as binary outcome) with hubs,
196 adjusting for sex, age and *APOE* ε4 genotype.

197 *Partial correlation network*

198 We used age, sex, *APOE* genotype, AD PRS (P_T = 0.1, *APOE* region excluded) and all hub
199 proteins/metabolites (with kME in the top 90th percentile) as input features for the graphical LASSO
200 algorithm and extended Bayesian information criterion to determine the model complexity for MCI
201 conversion using the R package `huge´ [23]. Data were auto-scaled prior to model-fitting. Partial
202 correlation network of selected metabolites, proteins and genetic variables was computed and
203 visualized with R package 'qgraph'.

204 *Mendelian randomization*

205 We finally investigated whether any of the A/T/N hubs correlating with MCI conversion status were
206 causally linked to AD, by performing bi-directional two-sample Mendelian Randomization (MR)
207 analyses implemented in the "TwoSampleMR" R package [24] and the MendelianRandomization
208 package [25]. A number of sensitivity analyses for both single cis instrument MR and multiple (cis)

instruments MR (**Supplementary methods**) were applied to determine the robustness of the MR findings.

3. Results

3.1. Subject demographics

Table 1 shows the demographic information of subjects for each individual omics analysis. Despite the difference in sample size for each omics layer analysis, no significant difference was observed in the distribution of sex across different diagnostic groups. However, the CTL group was younger and had a lower proportion of *APOE* ε4 carriers compared with the MCI and AD groups. Furthermore, the CTL participants had longer education and higher MMSE score. In terms of AD pathology markers, the ratio of abnormality of amyloid, P-tau and T-tau in AD and MCI individuals was, as expected, significantly higher than in controls.

Table 1. Demographics of participants included in multi-omics analysis by diagnosis. One-way analysis of variance (ANOVA) and chi-square tests were used to compare continuous and binary variables, respectively. Percentage of cases is shown in brackets for male sex, *APOE* ε4 carriers and the abnormality of amyloid, P-tau and T-tau.

Characteristics	Sample size	CTL	MCI	AD	*P* value
CSF proteomics					
n	371	123	154	94	NA
Age mean (SD), y	371	64.4 (7.8)	69.0 (7.4)	68.1 (8.1)	<0.001
Male sex N (%)	371	66 (54)	77 (50)	49 (52)	0.83
APOE ε4+ N (%)	371	45 (37)	78 (51)	59 (63)	<0.001
MMSE (SD)	370	28.7 (1.3)	26.5 (2.7)	22.1 (3.8)	<0.001
Education mean (SD), y	371	12.4 (3.5)	10.8 (3.6)	10.1 (3.8)	<0.001
Amyloid + N (%)	371	41 (33)	77 (50)	81 (86)	<0.001
P-tau + N (%)	367	29 (24)	87 (58)	69 (73)	<0.001
T-tau + N (%)	365	28 (23)	82 (55)	74 (80)	<0.001
Plasma proteomics					
n	972	372	409	191	NA
Age mean (SD), y	972	64.6 (8.0)	69.9 (8.0)	70.5 (8.8)	<0.001

Male sex N (%)	972	209 (56)	216 (53)	103 (54)	0.64
APOE ε4+ N (%)	972	139 (37)	195 (48)	116 (61)	<0.001
MMSE (SD)	967	28.8 (1.2)	26.2 (2.6)	21.4 (4.7)	<0.001
Education mean (SD), y	972	12.8 (3.7)	11.0 (3.7)	10.3 (3.9)	<0.001
Amyloid + N (%)	972	112 (30)	254 (62)	168 (88)	<0.001
P-tau + N (%)	876	53 (19)	215 (53)	128 (67)	<0.001
T-tau + N (%)	880	54 (19)	235 (58)	152 (80)	<0.001
Plasma metabolomics					
n	696	284	275	137	NA
Age mean (SD), y	696	65.0 (7.9)	70.0 (8.1)	70.1 (8.5)	<0.001
Male sex N (%)	696	155 (55)	141 (51)	81 (59)	0.60
APOE ε4+ N (%)	696	111 (39)	153 (56)	84 (61)	<0.001
MMSE (SD)	691	28.8 (1.1)	25.7 (2.8)	21.5 (4.8)	<0.001
Education mean (SD), y	696	12.8 (3.8)	11.1 (3.4)	10.4 (3.7)	<0.001
Amyloid + N (%)	696	114 (40)	197 (72)	122 (89)	<0.001
P-tau + N (%)	641	44 (19)	161 (59)	93 (68)	<0.001
T-tau + N (%)	641	45 (19)	177 (65)	107 (79)	<0.001

CTL, cognitively normal controls; MCI, mild cognitive impairment; AD, Alzheimer's disease; CSF, cerebrospinal fluid; SD, standard deviation; MMSE, mini mental state examination; +, abnormality; P-tau, phosphorylated tau; T-tau, total tau.

3.2 Co-expression network analysis of individual omics modalities reveals modules linked to AD endophenotypes

We first performed a clustering analysis of the CSF proteome using WGCNA. We found four modules (M) of co-expressed proteins. We ranked modules based on size from largest (M1 turquoise; n= 526 proteins) to smallest (M4 yellow; n=51 proteins) (**Figure 2A**, Table S1). We further investigated the biological significance of proteins in each module and found that three modules (M1 turquoise, M2 blue and M4 yellow modules) were enriched with various pathways after FDR correction (**Figure 2B**). When checking cell type enrichment, we found that all four modules were enriched with endothelial cells. Furthermore, M1 turquoise module was enriched with oligodendrocytes, neurons and astrocytes. M2 blue and M4 yellow modules were enriched with microglia (**Figure 2A**).

239 We then assessed the module correlations to AD endophenotypes. We used amyloid-β as "A", CSF P-
240 tau levels as a biomarker of tau ("T"), CSF T-tau as biomarkers of neurodegeneration ("N"), white
241 matter hyperintensity (WMH) volume as a biomarker for vascular disease burden ("V"), CSF YKL-40
242 as a biomarker of inflammation ("I") and MMSE score as "C" (**Figure 2A**). Overall, two (M1 and M4)
243 and three (M1, M2 and M3) modules were significantly associated with "T" and "N", respectively
244 after FDR correction. Furthermore, three (M1, M2 and M4) modules were associated with "I". None
245 of the modules were correlated with "A", "V", "C" or MCI conversion.

246 We used the same approach to analyse plasma proteomics and metabolomics data. We obtained
247 nine modules from plasma proteins (**Figure 2C,** previously published [26]). Four modules (M2, M3,
248 M4 and M8) had positive correlations with "A", "T" and "N". One (M3) and four (M1, M3, M8 and
249 M9) modules were associated with "V" and "I", respectively. In comparison, most plasma modules
250 were associated with "C" and MCI conversion. Furthermore, such associations were in concordance
251 with AT(N) markers correlations. For example, M2, M3, M4 and M8 modules were positively
252 associated with "A", "T" and "N" but were negatively correlated with MMSE score. Furthermore,
253 they were increased in MCI converters (n=103) compared with MCI non-converters (n=223) (**Figure**
254 **2C**). We further investigated the biological significance of proteins in four AT(N) markers-related
255 modules (M2, M3, M4 and M8) and found that three of them were enriched with various pathways,
256 such as cytokine-cytokine receptor interaction and metabolic pathways (**Figure 2D**).

257 For plasma metabolomics, we obtained seven modules (**Figure 2E**), among which M4 module was
258 negatively associated with "A", "T" and "N" and M3 module was positively associated with "N".
259 Furthermore, one (M1) and two (M1 and M4) modules were associated with "V" and "I",
260 respectively. Two (M3 and M4) and four (M1, M5, M6 and M7) modules were associated with "C"
261 and MCI conversion respectively. Furthermore, such associations were in concordance with AT(N)
262 markers correlations. We further investigated the biological significance of metabolites in AT(N)

263 markers-related modules (M3 and M4) and found that they were enriched in lipid pathways (**Figure**

264 **2F**).

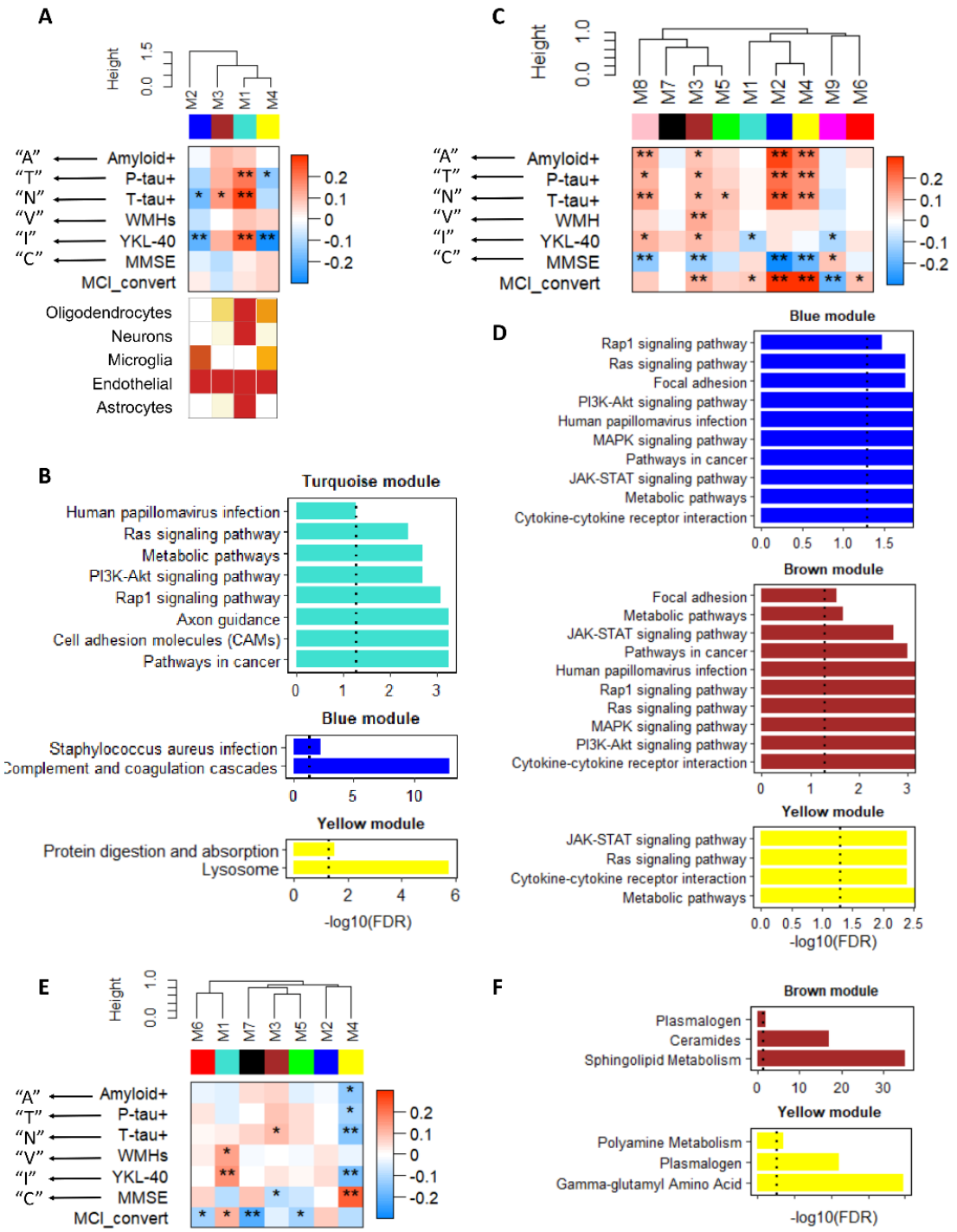

265 **Figure 2. Individual omics modules correlating to AD endophenotypes.** (A) Weighted gene
266 correlation network analysis (WGCNA) of the CSF proteomics and cell type enrichment analysis of
267 modules; (B) Enriched KEGG pathways of three modules in CSF proteins; (C) WGCNA of plasma
268 proteomics; (D) Enriched KEGG pathways of three modules in plasma proteins; (E) WGCNA of plasma

metabolomics; (F) Enriched KEGG pathways of two modules in plasma metabolites. * and ** denote significant correlations $p < 0.05$ and $p < 0.001$ after false discovery rate (FDR) correction respectively; CSF, cerebrospinal fluid; "A", amyloid; "T", tau; "N", neurodegeneration; "V", vascular; "I", inflammation; "C", cognition; +, abnormality; P-tau, phosphorylated tau; T-tau, total tau; WMH, white matter hyperintensity; MMSE, mini mental state examination; MCI, mild cognitive impairment.

3.3 Correlation of individual omics modules with the AT(N) framework

We dichotomized AT(N) biomarkers as normal or abnormal and categorized individuals into one of four groups: A-T-N- (no pathology), A+TN- (amyloid pathology), A+TN+ (Alzheimer pathology) and A-TN+ (SNAP). We then assessed the expression of each module eigenprotein/eigenmetabolite across different ATN groups. For CSF protein modules, we found that three modules (M1 turquoise, M2 blue and M4 yellow) showed a significant difference across ATN profiles from one-way ANOVA test (**Figure 3A-C**). Four plasma protein modules (M2 blue, M3 brown, M4 yellow and M8 pink, **Figure 3D-G,** adapted from [26]) and three plasma metabolites modules (M4 yellow, M5 green and M3 brown, **Figure 3H-J**) showed a significant difference across ATN profiles.

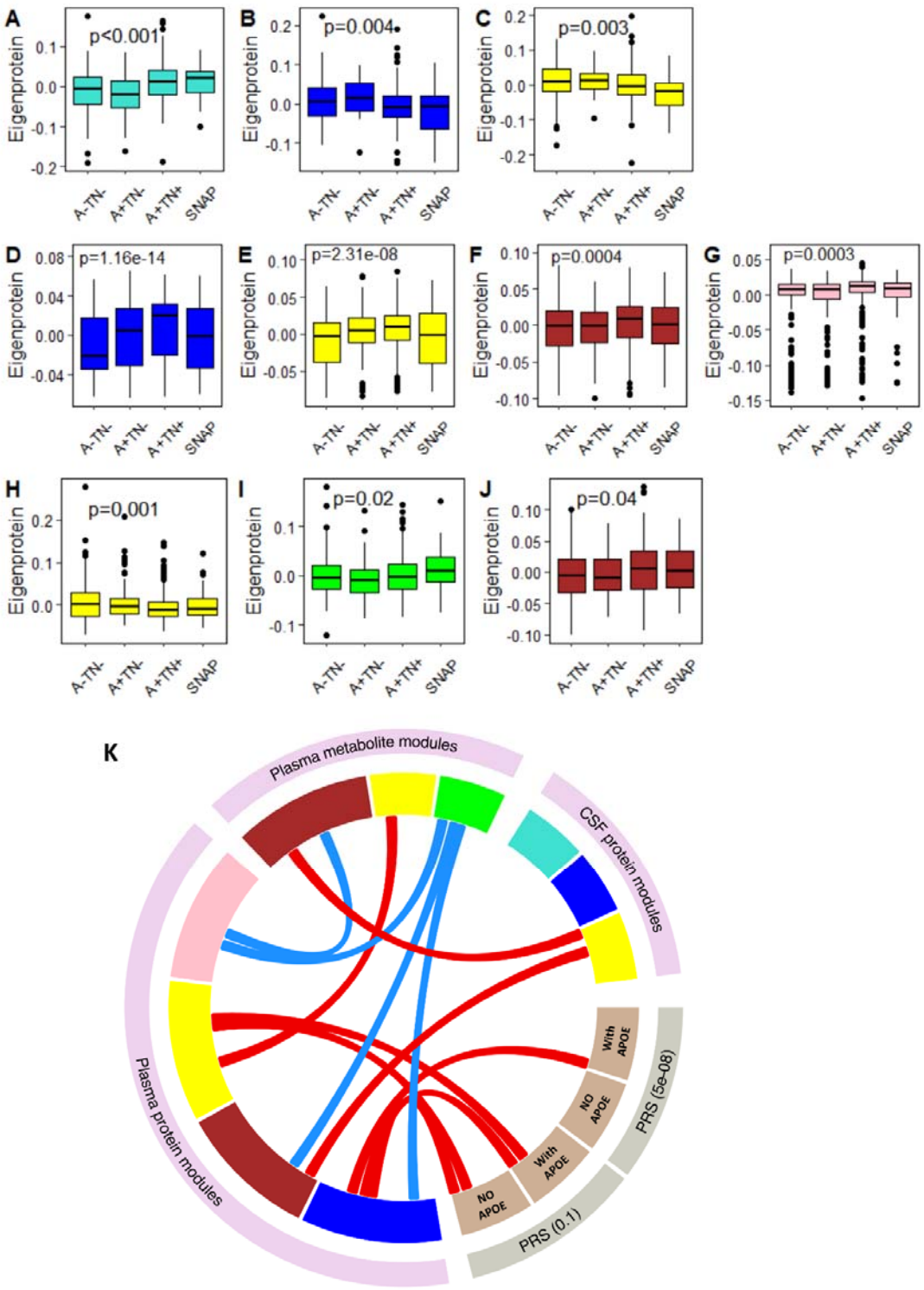

Figure 3. Protein and metabolite modules correlate to AT(N) profile and AD PRS. The relationship of the AT(N) framework with (A-C) three CSF protein modules, (D-G) four plasma protein modules, (H-J) three plasma metabolite modules, (K) Relation of AT(N) framework-related modules with AD PRS (with and without *APOE* region) at two thresholds (PT=$5x10^{-8}$ & 0.1); red and blue links denoted

288 positive and negative correlations, respectively. CSF, cerebrospinal fluid; SNAP, Suspected Non-
289 Alzheimer Pathology.

290 **3.4 Association between AT(N) framework-related modules and AD PRS**

291 We firstly selected AT(N) framework-related modules from each individual omics for further analysis.
292 As a result, we selected three CSF protein modules (M1 turquoise, M2 blue and M4 yellow), four
293 plasma protein modules (M2 blue, M3 brown, M4 yellow and M8 pink) and three plasma metabolite
294 modules (M3 brown, M4 yellow and M5 green). We then analysed the correlations between these
295 ten modules as well as between these modules and AD PRS. When analysing associations between
296 modules, we found that the metabolite M5 green module was negatively correlated with three
297 plasma protein modules (M2 blue, M3 brown and M8 pink). Additionally, a negative correlation was
298 observed between metabolite M3 brown module and plasma protein M8 pink module. In contrast, a
299 positive correlation was observed between metabolite M4 yellow module and plasma protein M4
300 yellow module as well as between metabolite M3 brown module and CSF protein M4 yellow module.
301 In addition, CSF protein M4 yellow module was positively associated with plasma protein M3 brown
302 module (**Figure 3K, Table S1-S3**).

303 When analysing the associations between these modules and AD PRS, we found that only plasma
304 protein modules were significantly associated with AD PRS. In detail, two plasma protein modules
305 (M2 blue and M4 yellow) were positively associated with PRS (*APOE* region included and excluded)
306 at P_T=0.1. Additionally, M2 blue module was significantly associated with PRS at $5x10^{-8}$ threshold
307 with *APOE* gene region included (**Figure 3K, Table S4**).

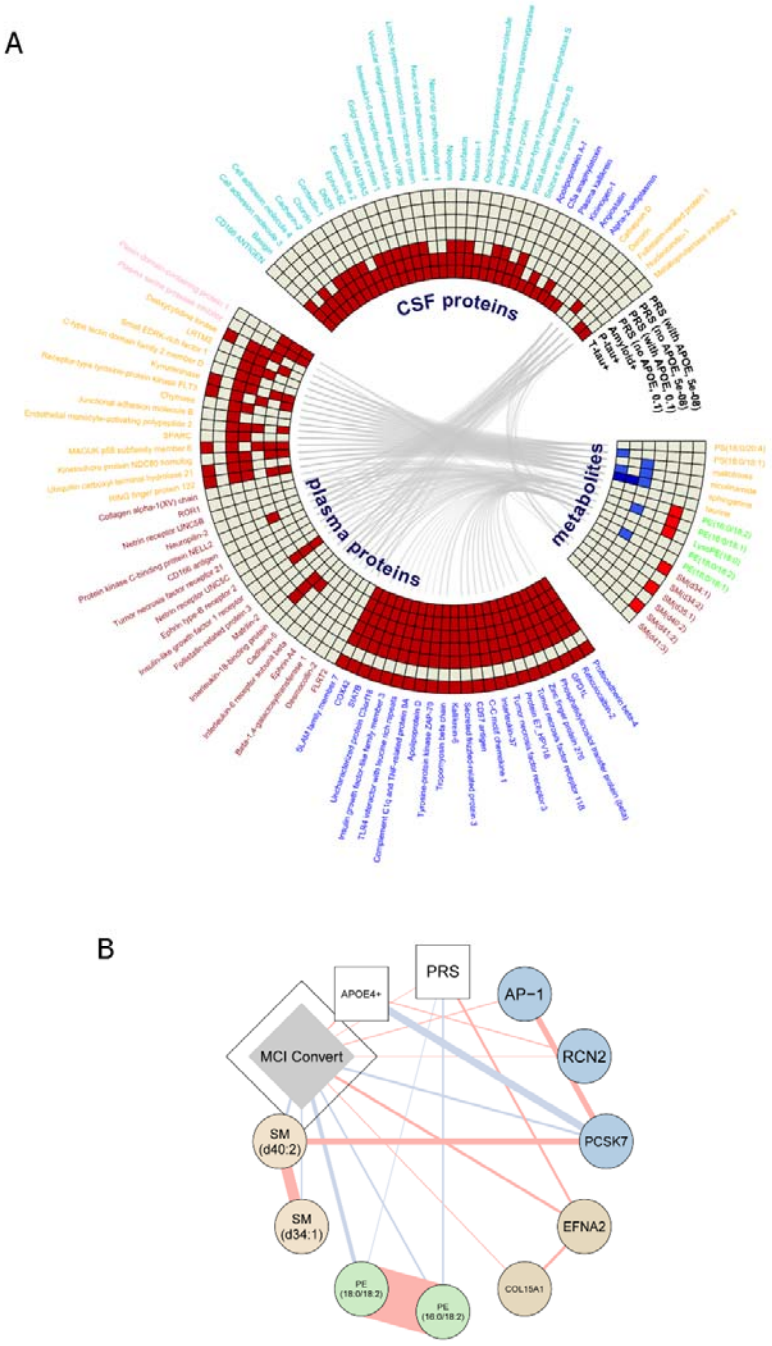

Figure 4. (A) Relation of hub proteins/metabolites with AT(N) markers and PRS; hub proteins/metabolites from three CSF protein modules (M1 turquoise, M2 blue and M4 yellow), four plasma protein modules (M2 blue, M3 brown, M4 yellow and M8 pink), and three plasma metabolite modules (M4 yellow, M5 green and M3 brown); red, blue, light red and light blue squares denoted

312 positive association at FDR level (*pFDR*<0.05), negative association at FDR level (*pFDR*<0.05), positive
313 association at nominal level (*p*<0.05, *pFDR*>0.05), and negative association at nominal level (*p*<0.05,
314 *pFDR*>0.05), respectively. **(B) Partial correlation network selected for hub metabolites/proteins,**
315 **genetic factors, and MCI conversion.** PRS, polygenic risk score; MCI, mild cognitive impairment.

316

317 **3.5 Association of hub proteins/metabolites with AT(N) markers and AD PRS**

318 We selected hub proteins/metabolites within AT(N) framework-related modules and analysed the
319 association between these hub proteins/metabolites (with kME varying from top 90th percentile to
320 top 98th percentile, **Table S5**), as well as the association of these hub proteins/metabolite with AT(N)
321 markers and AD PRS. When checking the associations between hub metabolites and proteins, we
322 found that there was a strong correlation between metabolites and plasma proteins. In detail, five
323 metabolites (four phosphatidylethanolamines (PEs) and one LysoPE) correlated with most hub
324 proteins after controlling for multiple testing. Two metabolites (sphingomyelins [SM] d40:2 and
325 d41:2) in M3 brown module were correlated with proteins in plasma M8 pink module and CSF M4
326 yellow module. In contrast, relatively week correlations were observed between CSF and plasma
327 proteins. (**Figure 4A, Table S6**).

328 We also investigated the association of these proteins/metabolites with AD PRS (*APOE* region
329 included and excluded (**Table S7**)). For plasma hub proteins, all 23 proteins in M2 blue module were
330 positively associated with AD PRS both at $P_T=5x10^{-8}$ (*APOE* region included) and $P_T=0.1$ (*APOE* region
331 included and excluded). Similar trend was also observed for most proteins in M4 yellow module,
332 with only six proteins being positively associated with AD PRS at $P_T=5x10^{-8}$ (*APOE* region included),
333 whereas most proteins, except for three, were associated with the $P_T=0.1$ AD PRS (with *APOE* and
334 without *APOE*) (**Figure 4A**). For hub metabolites, three SMs in M3 brown module and three PEs in
335 M5 green module were associated with AD PRS ($P_T=5x10^{-8}$) with and without *APOE* region
336 respectively. However, such associations did not pass FDR correction (**Figure 4A** in light red). No
337 associations were observed between CSF hub proteins and AD PRS.

338 When investigating the association of hub proteins and metabolites with AT(N) markers, we found
339 that most CSF and plasma hub proteins were positively associated with amyloid, P-tau and T-tau
340 after FDR correction. In contrast, hub metabolites were negatively associated with amyloid, P-tau
341 and T-tau only at nominal level except for sphinganine (**Figure 4A**) (**Table S8**).

342 **3.6 Hub molecules integration in MCI conversion**

343 Having demonstrated the association of hub proteins/metabolites with AT(N) markers and AD PRS,
344 we then sought to find a multimodal signal that might shed insights on MCI conversion. To do this
345 we first used LASSO algorithm and extended Bayesian information criterion to select features from
346 age, sex, AD PRS (P_T = 0.1, APOE region excluded), *APOE* ε4 genotype and all plasma hub
347 metabolites/proteins (with kME in the top 90th percentile, **Table S9**) to predict MCI conversion. As a
348 result, AD PRS, *APOE* ε4 genotype and several metabolites/proteins were selected from LASSO. Of
349 the metabolites/proteins, two SMs, two PEs and one protein (proprotein convertase subtilisin/kexin
350 type 7 [PCSK7]) from the blue module were negatively correlated with MCI conversion while the rest
351 four selected proteins were positively associated with MCI conversion including reticulocalbin 2
352 (RCN2) from the blue module, and three proteins from the brown module: ephrin receptor tyrosine
353 kinase A2 (EFNA2), Collagen alpha-1(XV) chain (COL15A1) and AP-1 complex subunit gamma-like 2
354 (AP-1) (**Figure 4B)**. In addition, correlations were also observed between metabolites/proteins and
355 AD PRS and *APOE* ε4 genotype (**Figure 4B**).

356 **3.7 Causal links of hub proteins/metabolites with AD**

357 We finally used a bidirectional two-sample Mendelian randomization to determine whether there
358 was evidence for a causal relationship of MCI conversion related hub proteins/metabolites with
359 Alzheimer's disease. Using Wald ratio estimate, we observed weak associations between PCSK7 and
360 AD as well as between COL15A1 and AD using data from Sun et al. [27]. In sensitivity analyses, the
361 causal relationship between PCSK7 and AD was replicated using summary data from an independent
362 protein GWA study by Suhre et al. [28] (**Table 2**). Further support for causal effects for the

363 association of PCSK7 with AD came from multiple-cis instrument MR (p<0.001 for IVW, 95% CI = 0.8
364 to 0.9, N_{SNPs} = 4, **Figure S1**), although this was not the case for COL15A1 (**Table S10**). Multiple-cis
365 instrument MR robust methods (MR-Egger and Weighted-median MR) and sensitivity analyses
366 estimates for PCSK7 were consistent with Wald ratio estimates in direction and magnitude, and
367 showed no horizontal pleiotropy or evidence of heterogeneity, further supporting the validity of the
368 MR assumptions (**Table S10**). In reverse MR analysis, we identified a causal association between
369 Alzheimer's disease, RCN2 and SM (**Table 2, Figure S2-3**). Robust methods and sensitivity analyses
370 provided additional support for such causal effects (**Table S10**).

371 **Table 2. Examination of the causal relationship between hub proteins/metabolites and**
372 **Alzheimer's using bidirectional Mendelian randomization**

Protein	Estimate*					
	Forward (hub proteins/metabolites →Alzheimer's disease)			Backward (Alzheimer's disease→ hub proteins/metabolites)		
	No. of SNPs	Slope (95% CI)	P value	No. of SNPs	Slope (95% CI)	P value
PCSK7	1 [27]	0.88 (0.79 - 0.99)	**0.029**	20	0.06 (-0.14 - 0.02)	0.135
PCSK7	1 [28]	0.96 (0.93 - 0.99)	**0.027**	NA	NA	NA
RCN2	1 [27]	1.04 (0.87 - 1.24)	0.648	20	0.10 (0.03 - 0.17)	**0.004**
EFNA2	1 [27]	1.04 (0.81 - 1.34)	0.741	20	-0.02 (-0.09 - 0.06)	0.679
AP-1	1 [27]	0.84 (0.67 - 1.04)	0.114	20	-0.01 (-0.09 - 0.07)	0.804
COL15A1	1 [27]	1.15 (1.01 - 1.30)	**0.032**	20	0.02 (-0.05 - 0.09)	0.544
SM	58 [29]	1.28 (0.87 - 1.89)	0.212**	21	0.14 (0.03 - 0.24) ***	**0.012**

373 *The Wald ratio estimate and inverse variance weighting (IVW) estimate were used for MR analyses with a
374 single and multiple SNPs, respectively.
375 ** Cochran's Q p<0.001
376 ***there was significant heterogeneity even after removing APOE (Cochran's Q p<0.05).
377

378 **4. Discussion (words:1161)**

379 Alzheimer's disease is characterized by non-linear and heterogeneous biological alterations. Multi-
380 level biological networks underlie AD pathophysiology, including but not limited to proteostasis
381 (amyloid-β and tau), synaptic homeostasis, inflammatory and immune responses, lipid and energy
382 metabolism, and oxidative stress [30]. Therefore, a systems-level approach is needed to fully capture
383 AD multifaceted pathophysiology. Here we used unbiased and high throughput multi-omics profiling
384 of AD. We applied correlation network analysis to identify modules linked to a variety of AD
385 endophenotypes including "A", "T", "N", "V", "I" and "C". We found that four modules obtained
386 from CSF proteins were associated with at least one pathology marker of "T" (P-tau), "N" (T-tau) and

387 “I” (YKL-40). Furthermore, the three “I” related modules (M1 turquoise, M2 blue and M4 yellow)
388 were enriched with either microglia or astrocytes, which are key cellular drivers and regulators of
389 neuroinflammation [31], further indicating the consistency between correlation network analysis
390 and cell type enrichment analysis. In addition, of the four modules, three were enriched with various
391 pathways which have been reported being associated with Alzheimer’s such as Ras signalling
392 pathway [32], axon guidance [33], cell adhesion molecules (CAMs) [34], and lysosome pathway [35],
393 further demonstrating the relatedness of these proteins with AD.

394 From plasma metabolomics, we found that the M3 brown module was associated with “N” (T-tau)
395 and “C” (cognition) and enriched with sphingolipid and ceramide metabolism. These findings align
396 with literature report as the lipids within this module have been reported being associated with
397 cognitive progression [36] and hippocampal atrophy [37]. In addition, M4 yellow module was
398 associated with five AD pathology markers (“A”, “T”, “N”, “I” and “C”) and enriched with three
399 pathways including gamma-glutamyl amino acid, plasmalogen, and polyamine metabolism. The
400 findings are also consistent with previous reports showing that these pathways were associated with
401 AD pathogenesis [38] and inflammatory cascade [39].

402 Two modules (M2 blue and M4 yellow) from plasma proteomics were associated with AD PRS (both
403 with and without *APOE* gene) at 0.1 level. Of the two modules, M2 blue module was associated with
404 PRS at $5x10^{-8}$ thresholds only when PRS included SNPs in the *APOE* region, indicating that such
405 association may be driven by *APOE*. Hub proteins in M2 blue module were correlated with PRS at
406 $5x10^{-8}$ thresholds only with SNPs in the *APOE* region included, further indicating that associations
407 may be driven by *APOE*. For plasma metabolomics, three sphingomyelins (SMs) from M3 brown
408 module were associated PRS ($P_T = 5x10^{-8}$) nominally only when the *APOE* region was included, also
409 indicating *APOE* gene dependence. This is in line with literature findings that nominal association
410 between SMs and PRS was reported [40].

411 We identified several closely correlated networks for metabolites, proteins, genetic factors, and MCI
412 conversion. Interestingly *APOE* and MCI conversion status were correlated to PCSK7 and
413 sphingomyelins SMs have been previously associated with cognitive progression in AD [41-43].
414 Furthermore, the integration of AD PRS showed that phosphatidylethanolamines [44, 45] and EFNA2
415 [46] were associated to both (MCI converter and AD PRS), with potential as early targets.

416 We finally investigated the causal relationship between A/T/N hubs associated with MCI conversion
417 status and AD. Our MR analyses highlighted a potential weak causal relationship between PCSK7 and
418 AD which was robust in both single and multiple cis instruments MR analyses and was replicated
419 using an independent pQTL dataset. We also found a causal relationship in the opposite direction,
420 whereby AD status is potentially causally linked to RCN2 that has been proposed as a therapeutic
421 target for atherosclerosis [47]. Finally, although we didn't have GWA summary data for the SM and
422 PE hubs examined in this study, our MR analyses showed that AD was causally linked to SM levels, as
423 previously shown when NMR data were used [48].

424 These findings are of great translational potential, particularly PCSK7 for which studies in Alzheimer's
425 disease are lacking. This convertase protein is very interesting as it is found in the BACE1 locus region
426 which encompasses several genes (PCSK7, RNF214, BACE1, CEP164) making it a plausible protein
427 activator of downstream amyloid deposition [49].

428 The causal associations from AD to RCN2 and sphingomyelins are also intriguing as both highlight a
429 possible vascular component caused by AD genetic liability, bringing new directionality between
430 vascular disease and dementia. These molecules and their potential causal links to AD suggest novel
431 avenues of research and intervention.

432 There are limitations for our study. First, the population in this study is of European ancestry and
433 mainly included participants who had high ratio of amyloid pathology and *APOE* ε4 carriers.
434 Therefore, they are not necessarily representative of the broader community. Validation in

435 independent cohorts and particularly in other ethnic groups and community-based populations are
436 needed to see if the results are generalizable.

437 Despite this, our study is the largest study we are aware of to report multi-omics relating to AD
438 endophenotypes, particularly to the AT(N) framework. Our findings offer new insights into changes
439 in individual proteins/metabolites linked to AD endophenotypes, the AT(N) framework and AD PRS.
440 The nominated causal proteins/metabolites may be tractable targets for mechanistic studies of AD
441 pathology. Furthermore, they may represent promising drug targets in the early stages of AD.

442

443 **Conflict of Interest**

444 SL is named as an inventor on biomarker intellectual property protected by Proteome Sciences and
445 Kings College London unrelated to the current study and within the past five years has advised for
446 Optum labs, Merck, SomaLogic and been the recipient of funding from AstraZeneca and other
447 companies via the IMI funding scheme. HZ has served at scientific advisory boards and/or as a
448 consultant for Abbvie, Alector, ALZPath, Annexon, Apellis, Artery Therapeutics, AZTherapies, CogRx,
449 Denali, Eisai, Nervgen, Novo Nordisk, Pinteon Therapeutics, Red Abbey Labs, reMYND, Passage Bio,
450 Roche, Samumed, Siemens Healthineers, Triplet Therapeutics, and Wave, has given lectures in
451 symposia sponsored by Cellectricon, Fujirebio, Alzecure, Biogen, and Roche, and is a co-founder of
452 Brain Biomarker Solutions in Gothenburg AB (BBS), which is a part of the GU Ventures Incubator
453 Program (outside submitted work). AL has served at scientific advisory boards of Fujirebio Europe, Eli
454 Lilly, Novartis, Nutricia and Otsuka and is the inventor of a patent on synaptic markers in CSF (all
455 unrelated to this study). JP has served at scientific advisory boards of Fujirebio Europe, Eli Lilly and
456 Nestlé Institute of Health Sciences, all unrelated to this study. SE has received unrestricted research
457 grants from Janssen Pharmaceutica and ADx Neurosciences and has served at scientific advisory
458 boards of Biogen, Eisai, Novartis, Nutricia / Danone, all unrelated to this study. FB is a steering
459 committee or iDMC member for Biogen, Merck, Roche, EISAI and Prothena. Consultant for Roche,

460 Biogen, Merck, IXICO, Jansen, Combinostics. Research agreements with Merck, Biogen, GE
461 Healthcare, Roche. Co-founder and shareholder of Queen Square Analytics LTD, all unrelated to this
462 study.

463 **Acknowledgements**

464 This research was conducted as part of the EMIF-AD MBD project which has received support from
465 the Innovative Medicines Initiative Joint Undertaking under EMIF grant agreement no 115372,
466 resources of which are composed of financial contribution from the European Union's Seventh
467 Framework Programme (FP7/2007-2013) and EFPIA companies' in-kind contribution. The DESCRIPA
468 study was funded by the European Commission within the 5th framework program (QLRT-2001-
469 2455). The EDAR study was funded by the European Commission within the 5th framework program
470 (contract # 37670). The Leuven cohort was funded by the Stichting voor Alzheimer Onderzoek (grant
471 numbers #11020, #13007 and #15005). RV is a senior clinical investigator of the Flemish Research
472 Foundation (FWO). The San Sebastian GAP study is partially funded by the Department of Health of
473 the Basque Government (allocation 17.0.1.08.12.0000.2.454.01.41142.001.H). We acknowledge the
474 contribution of the personnel of the Genomic Service Facility at the VIB-U Antwerp Center for
475 Molecular Neurology. The research at VIB-CMN is funded in part by the University of Antwerp
476 Research Fund. HZ is a Wallenberg Scholar supported by grants from the Swedish Research Council
477 (#2018-02532), the European Research Council (#681712), Swedish State Support for Clinical
478 Research (#ALFGBG-720931), the Alzheimer Drug Discovery Foundation (ADDF), USA (#201809-
479 2016862), and the UK Dementia Research Institute at UCL. FB is supported by the NIHR biomedical
480 research centre at UCLH. LS is funded by the Virtual Brain Cloud from European commission (grant
481 no. H2020-SC1-DTH-2018-1). R.G. was supported by the National Institute for Health Research (NIHR)
482 Biomedical Research Centre at South London and Maudsley NHS Foundation Trust and King's College
483 London. This paper represents independent research part-funded by the National Institute for
484 Health Research (NIHR) Biomedical Research Centre at South London and Maudsley NHS Foundation

Trust and King's College London. The views expressed are those of the author(s) and not necessarily those of the NHS, the NIHR or the Department of Health and Social Care. JX and CLQ thank Lundbeck Fonden for the support.

Ethics Statement

Written informed consent was obtained from all participants before inclusion in the study. The medical ethics committee at each site approved the study.

Data Availability

The datasets generated and analysed during the current study are available from the EMIF-AD Catalogue via submitted research proposals which have to be approved by the data-owners from each parent cohort.

References

1. Knopman, D.S., et al., *Alzheimer disease.* Nat Rev Dis Primers, 2021. **7**(1): p. 33.
2. Jack, C.R., Jr., et al., *NIA-AA Research Framework: Toward a biological definition of Alzheimer's disease.* Alzheimers Dement, 2018. **14**(4): p. 535-562.
3. Johnson, E.C.B., et al., *Large-scale proteomic analysis of Alzheimer's disease brain and cerebrospinal fluid reveals early changes in energy metabolism associated with microglia and astrocyte activation.* Nat Med, 2020. **26**(5): p. 769-780.
4. Higginbotham, L., et al., *Integrated proteomics reveals brain-based cerebrospinal fluid biomarkers in asymptomatic and symptomatic Alzheimer's disease.* Sci Adv, 2020. **6**(43).
5. Butterfield, D.A. and D. Boyd-Kimball, *Oxidative Stress, Amyloid-β Peptide, and Altered Key Molecular Pathways in the Pathogenesis and Progression of Alzheimer's Disease.* J Alzheimers Dis, 2018. **62**(3): p. 1345-1367.
6. Ashton, N.J., et al., *Blood protein predictors of brain amyloid for enrichment in clinical trials?* Alzheimers Dement (Amst), 2015. **1**(1): p. 48-60.
7. Hye, A., et al., *Plasma proteins predict conversion to dementia from prodromal disease.* Alzheimers Dement, 2014. **10**(6): p. 799-807.e2.
8. Shi, L., et al., *Discovery and validation of plasma proteomic biomarkers relating to brain amyloid burden by SOMAscan assay.* Alzheimers Dement, 2019. **15**(11): p. 1478-1488.
9. Wilkins, J.M. and E. Trushina, *Application of Metabolomics in Alzheimer's Disease.* Front Neurol, 2017. **8**: p. 719.
10. Tönnies, E. and E. Trushina, *Oxidative Stress, Synaptic Dysfunction, and Alzheimer's Disease.* J Alzheimers Dis, 2017. **57**(4): p. 1105-1121.
11. Kim, M., et al., *Primary fatty amides in plasma associated with brain amyloid burden, hippocampal volume, and memory in the European Medical Information Framework for Alzheimer's Disease biomarker discovery cohort.* Alzheimers Dement, 2019. **15**(6): p. 817-827.
12. Bos, I., et al., *The EMIF-AD Multimodal Biomarker Discovery study: design, methods and cohort characteristics.* Alzheimers Res Ther, 2018. **10**(1): p. 64.

522 13. Tijms, B.M., et al., *Pathophysiological subtypes of Alzheimer's disease based on cerebrospinal*
523 *fluid proteomics.* Brain, 2020. **143**(12): p. 3776-3792.
524 14. Shi, L., et al., *Discovery and validation of plasma proteomic biomarkers relating to brain*
525 *amyloid burden by SOMAscan assay.* Alzheimer's & Dementia, 2019. **15**(11): p. 1478-1488.
526 15. Hong, S., et al., *Genome-wide association study of Alzheimer's disease CSF biomarkers in the*
527 *EMIF-AD Multimodal Biomarker Discovery dataset.* Transl Psychiatry, 2020. **10**(1): p. 403.
528 16. Langfelder, P. and S. Horvath, *WGCNA: an R package for weighted correlation network*
529 *analysis.* BMC Bioinformatics, 2008. **9**: p. 559.
530 17. Xu, J., et al., *Sex-Specific Metabolic Pathways Were Associated with Alzheimer's Disease (AD)*
531 *Endophenotypes in the European Medical Information Framework for AD Multimodal*
532 *Biomarker Discovery Cohort.* Biomedicines, 2021. **9**(11).
533 18. Kunkle, B.W., et al., *Genetic meta-analysis of diagnosed Alzheimer's disease identifies new*
534 *risk loci and implicates Aβ, tau, immunity and lipid processing.* Nat Genet, 2019. **51**(3): p.
535 414-430.
536 19. Euesden, J., C.M. Lewis, and P.F. O'Reilly, *PRSice: Polygenic Risk Score software.*
537 Bioinformatics, 2015. **31**(9): p. 1466-8.
538 20. Zettergren, A., et al., *Association between polygenic risk score of Alzheimer's disease and*
539 *plasma phosphorylated tau in individuals from the Alzheimer's Disease Neuroimaging*
540 *Initiative.* Alzheimers Res Ther, 2021. **13**(1): p. 17.
541 21. Leonenko, G., et al., *Identifying individuals with high risk of Alzheimer's disease using*
542 *polygenic risk scores.* Nat Commun, 2021. **12**(1): p. 4506.
543 22. Hong, S., et al., *TMEM106B and CPOX are genetic determinants of cerebrospinal fluid*
544 *Alzheimer's disease biomarker levels.* Alzheimers Dement, 2021. **17**(10): p. 1628-1640.
545 23. Tofte, N., et al., *Metabolomic Assessment Reveals Alteration in Polyols and Branched Chain*
546 *Amino Acids Associated With Present and Future Renal Impairment in a Discovery Cohort of*
547 *637 Persons With Type 1 Diabetes.* Front Endocrinol (Lausanne), 2019. **10**: p. 818.
548 24. Hemani, G., et al., *The MR-Base platform supports systematic causal inference across the*
549 *human phenome.* Elife, 2018. **7**.
550 25. Yavorska, O.O. and S. Burgess, *MendelianRandomization: an R package for performing*
551 *Mendelian randomization analyses using summarized data.* Int J Epidemiol, 2017. **46**(6): p.
552 1734-1739.
553 26. Shi, L., et al., *Replication study of plasma proteins relating to Alzheimer's pathology.*
554 Alzheimers Dement, 2021. **17**(9): p. 1452-1464.
555 27. Sun, B.B., et al., *Genomic atlas of the human plasma proteome.* Nature, 2018. **558**(7708): p.
556 73-79.
557 28. Suhre, K., et al., *Connecting genetic risk to disease end points through the human blood*
558 *plasma proteome.* Nat Commun, 2017. **8**: p. 14357.
559 29. Borges, M.C., et al., *Circulating Fatty Acids and Risk of Coronary Heart Disease and Stroke:*
560 *Individual Participant Data Meta-Analysis in Up to 16 126 Participants.* J Am Heart Assoc,
561 2020. **9**(5): p. e013131.
562 30. Hampel, H., et al., *Omics sciences for systems biology in Alzheimer's disease: State-of-the-art*
563 *of the evidence.* Ageing Res Rev, 2021. **69**: p. 101346.
564 31. Hampel, H., et al., *A Path Toward Precision Medicine for Neuroinflammatory Mechanisms in*
565 *Alzheimer's Disease.* Front Immunol, 2020. **11**: p. 456.
566 32. Kirouac, L., et al., *Activation of Ras-ERK Signaling and GSK-3 by Amyloid Precursor Protein*
567 *and Amyloid Beta Facilitates Neurodegeneration in Alzheimer's Disease.* eNeuro, 2017. **4**(2).
568 33. Zhang, L., et al., *Roles and Mechanisms of Axon-Guidance Molecules in Alzheimer's Disease.*
569 Mol Neurobiol, 2021. **58**(7): p. 3290-3307.
570 34. Nagappan-Chettiar, S., E.M. Johnson-Venkatesh, and H. Umemori, *Activity-dependent*
571 *proteolytic cleavage of cell adhesion molecules regulates excitatory synaptic development*
572 *and function.* Neurosci Res, 2017. **116**: p. 60-69.

573 35. Zhang, Y., et al., *The role of ubiquitin proteasomal system and autophagy-lysosome pathway*
574 *in Alzheimer's disease.* Rev Neurosci, 2017. **28**(8): p. 861-868.
575 36. Kalinichenko, L.S., et al., *Sphingolipid control of cognitive functions in health and disease.*
576 Prog Lipid Res, 2022. **86**: p. 101162.
577 37. Kim, M., et al., *Association between Plasma Ceramides and Phosphatidylcholines and*
578 *Hippocampal Brain Volume in Late Onset Alzheimer's Disease.* J Alzheimers Dis, 2017. **60**(3):
579 p. 809-817.
580 38. Mahajan, U.V., et al., *Dysregulation of multiple metabolic networks related to brain*
581 *transmethylation and polyamine pathways in Alzheimer disease: A targeted metabolomic*
582 *and transcriptomic study.* PLoS Med, 2020. **17**(1): p. e1003012.
583 39. Bozelli, J.C., Jr., S. Azher, and R.M. Epand, *Plasmalogens and Chronic Inflammatory Diseases.*
584 Front Physiol, 2021. **12**: p. 730829.
585 40. Liu, Y., et al., *Plasma lipidome is dysregulated in Alzheimer's disease and is associated with*
586 *disease risk genes.* Transl Psychiatry, 2021. **11**(1): p. 344.
587 41. Mielke, M.M., et al., *Plasma sphingomyelins are associated with cognitive progression in*
588 *Alzheimer's disease.* J Alzheimers Dis, 2011. **27**(2): p. 259-69.
589 42. He, X., et al., *Deregulation of sphingolipid metabolism in Alzheimer's disease.* Neurobiol
590 Aging, 2010. **31**(3): p. 398-408.
591 43. Morrow, A.R., et al., *CSF sphingomyelin metabolites in Alzheimer's disease,*
592 *neurodegeneration, and neuroinflammation.* Alzheimer's & Dementia, 2021. **17**: p. e052290.
593 44. Llano, D.A. and V. Devanarayan, *Serum Phosphatidylethanolamine and*
594 *Lysophosphatidylethanolamine Levels Differentiate Alzheimer's Disease from Controls and*
595 *Predict Progression from Mild Cognitive Impairment.* J Alzheimers Dis, 2021. **80**(1): p. 311-
596 319.
597 45. Calzada, E., O. Onguka, and S.M. Claypool, *Phosphatidylethanolamine Metabolism in Health*
598 *and Disease.* Int Rev Cell Mol Biol, 2016. **321**: p. 29-88.
599 46. Ma, X., et al., *Metabolic Reprogramming of Microglia Enhances Proinflammatory Cytokine*
600 *Release through EphA2/p38 MAPK Pathway in Alzheimer's Disease.* J Alzheimers Dis, 2022.
601 47. Li, J., et al., *Reticulocalbin 2 as a Potential Biomarker and Therapeutic Target for*
602 *Atherosclerosis.* Cells, 2022. **11**(7).
603 48. Compton, H., et al., *Effects of genetic liability to Alzheimer's disease on circulating*
604 *metabolites across the life course.* medRxiv, 2022: p. 2022.03.24.22272867.
605 49. Damotte, V., et al., *Plasma amyloid β levels are driven by genetic variants near APOE, BACE1,*
606 *APP, PSEN2: A genome-wide association study in over 12,000 non-demented participants.*
607 Alzheimers Dement, 2021. **17**(10): p. 1663-1674.

608